HHS Public Access

Author manuscript

J Cardiovasc Comput Tomogr. Author manuscript; available in PMC 2020 February 21.

Published in final edited form as:

J Cardiovasc Comput Tomogr. 2012 ; 6(1): 14–23. doi:10.1016/j.jcct.2011.10.014.

Infarct detection with a comprehensive cardiac CT protocol

Brian B. Ghoshhajra, MD, MBA[#a], **Pal Maurovich-Horvat, MD**[#a], **Tust Techasith, BS**[a], **Hector M. Medina, MD**[a], **Daniel Verdini, MD**[a], **Manavjot S. Sidhu, MD**[a,*], **Ron Blankstein, MD**[b], **Thomas J. Brady, MD**[a], **Ricardo C. Cury, MD**[a,c]

[a]Cardiac MR PET CT Program, Department of Radiology and Division of Cardiology, Massachusetts General Hospital and Harvard Medical School, 165 Cambridge Street, Suite 400, Boston, MA 02114, USA;

[b]Non-Invasive Cardiovascular Imaging Program, Cardiovascular Division and Department of Radiology, Brigham and Women's Hospital, Boston, MA, USA

[c]Cardiovascular MRI and CT Program, Baptist Cardiac and Vascular Institute, Miami, FL, USA

[#] These authors contributed equally to this work.

Abstract

BACKGROUND: Cardiac CT has the potential to offer comprehensive infarct detection by assessing regional wall motion abnormalities (RWMAs), rest perfusion defects (RPDs), and delayed contrast enhancement (DCE). However, the diagnostic accuracy of these techniques for the detection of myocardial infarction (MI) is unknown.

METHODS: Forty-eight patients with intermediate-to-high probability for coronary artery disease after single-photon emitting CT myocardial perfusion imaging were prospectively enrolled for a research comprehensive 64-detector row dual-source cardiac CT protocol that included cine images for RWMA, first-pass images for RPD, and delayed images for DCE. Blinded readers independently assessed each technique. Subsequently, a final combined analysis (cine 1 rest 1 DCE) was performed. The universal definition for MI by the 2007 American Heart Association task force was used as the "gold standard."

RESULTS: Twenty-four of 48 patients (50%) had infarct by the universal definition. The combined CT analysis was most accurate (90%) with the highest per-patient sensitivity (88%) and specificity (92%) versus individual assessments (RWMA, 79% and 88%; RPD, 67% and 92%; DCE, 79% and 88%). Similar findings were observed on a per-vessel basis analysis. A combination of DCE and cine showed a good accuracy (85%) and high sensitivity (92%).

CONCLUSIONS: Infarct detection with CT is feasible with overall good diagnostic accuracy compared with the universal definition. A combined evaluation that included all techniques (cine, RPD, and DCE) had the highest diagnostic accuracy. These findings may have implications when designing future clinical and research CT protocols for optimal infarct detection.

[*]Corresponding author. msidhu1@partners.org.

Conflict of interest: The authors report no conflicts of interest.

Keywords

Diagnostic imaging; Cardiovascular disease; Myocardial perfusion; Myocardial infarction; X-ray computed tomography; Myocardial perfusion imaging; Cardiac-gated imaging techniques

Introduction

Cardiac CT angiography (CTA) is most frequently performed to assess the presence of coronary artery disease (CAD) and to exclude significant stenosis. The modality shows excellent sensitivity and negative predictive value in patients with low-to-intermediate pretest probability for CAD.[1,2] Although the utility of CTA to exclude obstructive CAD in selected patient populations is excellent, the recently reported capabilities of CT to assess myocardial enhancement patterns has moved cardiac CT beyond the realm of a simple angiographic examination. CT perfusion (CTP) is a technique that has been shown to detect myocardial infarcts (MIs) compared with single-photon emission computed tomography myocardial perfusion imaging (SPECT-MPI), particularly during rest CT studies.[3] CTP has also shown the ability to identify reversible myocardial perfusion defects (myocardial ischemia) by imaging during contrast injection under pharmacologic stress.[4,5]

Gated cardiac CT offers the ability to obtain cine functional images for assessment of global left ventricular (LV) function and detection of regional wall motion abnormalities (RWMAs),[6,7] myocardial perfusion images for detection of perfusion defects,[8,9] and delayed contrast enhancement (DCE) images for detection of delayed hyperenhancement.[10–14] Moreover, CT has long offered the ability to detect signs of remote myocardial infarction (such as wall thinning, fatty metaplasia, and myocardial calcifications).[15–19] Although many of these CT techniques have been previously studied independently, the combined accuracy of these phases in a single comprehensive examination has not been studied. Most of these features can also be assessed with cardiac magnetic resonance imaging (MRI), a well-established technique for MI detection.[20–24] The advent of dual-source cardiac CT has allowed acquisitions to be obtained at high heart rates and with improved temporal resolution.[25–27]

We performed a comprehensive cardiac CT examination as part of an initial feasibility study of CTP and sought to determine the accuracy of each component of this protocol (CTP, DCE, and cine) versus the current clinical imaging standard, SPECT-MPI, as well as using a clinical reference standard (taking into account all available patient information), according to the American Heart Association (AHA) “universal definition” of MI.[28] We sought to test the hypothesis that a comprehensive protocol that used multiple phases of CT acquisition (CTP, DCE, and cine) would be more accurate for detecting myocardial infarction than each individual acquisition and that delayed images would have the highest accuracy compared with CTP and cine images.

Methods

Images were obtained as part of a feasibility trial in which patients underwent myocardial CTP, including delayed enhancement images with dual-source, electrocardiogram (ECG)–

gated technique. Most patients also had invasive coronary angiography (ICA). Our institutional review board approved the study protocol. Written informed consent was obtained before subject enrollment. Compliance with the Health Insurance Portability and Accountability Act was maintained. The stress perfusion component of the data was reported previously in separate analyses of a smaller series of patients used to evaluate the feasibility and accuracy of stress CTP compared with quantitative coronary angiography and SPECT-MPI,[4] the incremental value of stress CTP compared with CTA,[29] and the interscan reliability of stress CTP compared with SPECT MPI.[3] Astellas Pharma (Deerfield, IL) provided partial support, supplying the adenosine and research grant support. The authors maintained full control of the data and performed the statistical analysis.

Study subjects

In this study, a cohort of 48 patients was prospectively enrolled as part of a research protocol to test the feasibility and diagnostic accuracy of CTP in a population with moderate-to-high risk of CAD. Inclusion criteria were patients with an intermediate-to-high likelihood of CAD and who also had a SPECT study within 60 days of the CTP. Exclusion criteria were acute coronary syndrome, decompensated heart failure, advanced heart block, asthma, critical aortic stenosis, systolic blood pressure, < 90 mm Hg, known allergy to iodinated contrast, serum creatinine. > 1.5 mg/dL, pregnancy, and atrial fibrillation. Patient characteristics are listed in Table 1.

Myocardial CT viability protocol

Comprehensive cardiac CT was performed with a first-generation 64-slice dual-source scanner (Somatom Definition; Siemens Medical Solutions, Forchheim, Germany). An intravenous catheter was placed in the right antecubital vein for contrast injection. A second intravenous catheter was placed in the left antecubital fossa for injection of adenosine for pharmacologic stress perfusion imaging, as was analyzed and reported previously.[4]

After scout images, adenosine infusion was initiated at a rate of 140 μg/mL. After 1 minute, contrast timing was determined by test bolus injection, with a region of interest in the proximal ascending aorta, as follows: 10–15 mL of contrast (370 mg of iopamidol/mL; Isovue-370; Bracco Diagnostics, Princeton, NJ) at 4 mL/s, followed by 20-mL saline flush. After ≥3 minutes of adenosine infusion, stress phase retrospective acquisition was performed. Iopamidol was injected at 4–5 mL/s according to the scanning duration (mean, 65.8 mL). Cardiac CT was acquired from the carina to the diaphragm with helical-mode retrospective ECG gating. Images were acquired at 2 × 32 × 0.6 mm (number of x-ray sources × number of detector slices × slice thickness) with the use of a gantry rotation time of 330 milliseconds with a half-scan reconstruction algorithm (temporal resolution, 83 milliseconds). A z-flying focal spot was used in retrospective-gated modes to acquire 64 overlapping slices per rotation with a sampling distance of 0.3 mm at the isocenter. The tube voltage was selected according to the body mass index (BMI): 100 kV for BMI, < 30 kg/m^2 and 120 kV for BMI ≥ 30 kg/m^2. Tube current was varied from 230 to 370 mA according to patient size. ECG-based tube current modulation was implemented with a pulsing window of 60%–70% of the R-R interval for peak reference milliampere, and 20% of the peak

reference milliampere for the remainder of the R-R cycle. Automatic heart rate–based adaptive pitch selection (0.2–0.5) was enabled.

These cine images were reconstructed at 5% R-R intervals and used for assessment of global and regional LV function and structure and particularly for detection of RWMAs. In prior trials, stress myocardial perfusion and coronary CTA were also assessed during this acquisition.[4]

Approximately 5 minutes later, a rest phase, axial-mode prospectively ECG-triggered acquisition centered at 65% of the R-R interval was then performed with a tube current varying from 150 to 258 mA, based on patient size and a section thickness of 0.75 mm (collimation, 32 × 0.75 mm). The same tube voltage (100 or 120 kV) and approximately the same contrast material volume were used for the first and second image acquisitions. In some cases, rest acquisition required ≤70 mL of contrast (mean, 62.2 mL) to allow for a longer scan time because of table movement and ECG synchronization to every second heartbeat.

Approximately 10–15 minutes after the initial contrast-enhanced CTA, a third, delayed phase acquisition was performed (Fig. 1). There was an average of 13 minutes, 16 seconds between initial contrast administration and acquisition of the delayed images. An axial-mode prospectively ECG-triggered acquisition centered at 65% of the R-R interval was performed with a tube current varying from 150 to 258 mA, a tube voltage of 100kV, and a section thickness of 1.2 mm (collimation, 19 × 1.2 mm). No additional contrast was given during this acquisition. Radiation dose recorded for the protocol includes all 3 acquisitions, scout views, and test bolus images. Total radiation dose is mentioned as dose-length product (DLP).

Data analysis

Two experienced investigators (B.B.G. and R.C.C.) independently analyzed each component of the cardiac CT datasets in blinded fashion. Images were interpreted on an independent workstation. Readers were provided only the short-axis images and allowed to adjust the window width and window level to their own preference. DCE, rest perfusion, and cine image sets were each assessed separately with a random order of patients that varied between the image sets. A final combined read that all 3 phases of imaging (delayed, rest perfusion, and cine images) was performed. The American College of Cardiology (ACC) AHA 17-segment model for standardized myocardial segmentation was used for image interpretation.[30]A joint consensus reading session was then performed to resolve any discrepancies, and consensus was achieved in all cases.

Image analysis for the detection of wall motion abnormality—Cine loops were visualized in the short-axis (basal, mid, apical), 2-chamber, and 4-chamber views. Wall motion was rated as normal, hypokinetic, akinetic, and dyskinetic. Structural abnormalities, including myocardial thinning, calcification, and fatty metaplasia, were also recorded.

Image analysis for the detection of rest perfusion defect—Rest-phase CT scans were reconstructed by multiplanar reformation in the short-axis view with a slice thickness

of 8 mm. A smooth to medium-smooth convolution kernel (B26f or B30f) was applied. The LV myocardium was assessed for the presence of rest perfusion defect (RPD). Degree of perfusion defect was rated on a 4-point scale (0 = no perfusion defect, 1 = mild defect, 2 = moderate defect, 3 = severe defect). For any perfusion defect (1–3), the transmurality was rated on a 3-point scale (1 = defect is subendocardial only, 2 = defect extends into myocardium, 3 = transmural).

Image analysis for the detection of DCE—Delayed-phase dual-source CT scans were reconstructed in similar fashion to the rest-phase scan above. The LV myocardium was assessed for the presence of local DCE. Degree was rated on a 4-point scale (0 = no DCE, 1 = mild DCE, 2 = moderate DCE, 3 = severe DCE), and the transmurality was rated on a 3-point scale (1 = defect is subendocardial only, 2 = defect extends into myocardium, 3 = defect is transmural).

Image analysis for combinations of techniques—Combinations of CT techniques were evaluated with the use of the “believe the positive” rule, meaning that the overall test result, combining for example rest and delayed images, was positive if the result of ≥1 of the tests (rest or delayed) was positive. If both tests were negative, the overall test result was negative.

Combined analysis

All available scans were viewed in total for a final, combined analysis. Readers were provided sets of the cine, rest perfusion, and DCE series, as well as the results of their prior individual phase readings. The reader then was given the opportunity to form an impression on the basis of all available imaging, rather than only a single phase.

Image quality and confidence—Image quality (IQ) and confidence levels (CLs) were subjectively rated by the readers on a 4-point scale (IQ: 1 = poor, 2 = good, 3 = very good, 4 = excellent; CL: 1 = no confidence, 2 = low confidence, 3 = intermediate confidence, 4 = high confidence).

Quantification of DCE—DCE was defined as regions of increased signal intensity compared with normal remote myocardium (myocardium with no evidence of wall thinning, fatty infiltration, or calcification), and with a mean difference of ≥20 HU. DCE was measured with regions of interest placed within the hyperenhanced regions. Regions of interest were also measured in remote myocardium and in the LV cavity. The contrast-to-noise ratio (CNR) was calculated with a previously described method.[31]

Reference standard—All available clinical history, ECG, SPECT (n = 48), ICA (n = 39), and echocardiography (n = 34) were reviewed independently of CT results for final MI adjudication according to the 2007 AHA Task Force universal definition of MI.[28] Non-CT imaging results were recorded by myocardial segment to compare with CT segmental readings. The reference standard was adjudicated in an independent and blinded fashion by 2 trained cardiologists (H.M.M. and R.B.) who were blinded to the CT findings.

Statistical analysis

Continuous variable data are reported as means ± SDs, and categorical variable data are presented as percentages. Differences between continuous variables were assessed by *t* tests, and differences between categorical variables were assessed by chi-square tests. The diagnostic accuracy of various CT phases for the detection of infarction, using the reference MI as a standard, was expressed as sensitivity, specificity, positive predictive value, negative predictive value, and accuracy with a corresponding binomial 95% CL. Calculations were performed on both a per-vessel (left anterior descending, left circumflex, and right coronary arteries) and per-patient basis. JMP software (SAS Institute Inc, Cary, NC) was used for statistical analysis.

Results

Patient characteristics

Patient characteristics are summarized in Table 1. A total of 24 of 48 patients (50%) included in the cohort had a final diagnosis of MI by the universal AHA definition. The difference in mean age between patients with and without evidence of reference MI (63.3 ± 10.2 and 61.2 ± 11.0, respectively; $P = 0.35$) was not significant. Patients with reference MI tended to be male and were likely to have dyslipidemia, reported history of MI, prior revascularization, and history of statin use.

Diagnostic accuracy

On a per-patient basis (Table 2), the diagnostic accuracy of our CT viability protocol for infarct detection versus the reference standard was 90% for the combined read. Individually, DCE and cine images each had an accuracy of 83%, whereas rest images had an accuracy of 79%. The sensitivity of rest images was 67% compared with 79% for both DCE and cine images. Of the individual phases, rest images had the highest specificity at 92%. When comparing combinations of techniques and applying the believe the positive rule, a combination of DCE and cine images showed the highest sensitivity (92%) compared with the other two combinations (83%) and had the highest accuracy (85% vs 83%, 81%).

On a per-vessel basis (Table 2), the diagnostic accuracy of the CT viability protocol for infarct versus the reference standard was 83% (the combined reading with all images). This was similar to the accuracies of individually interpreted DCE (82%), rest (81%), and cine (82%) images. Similar accuracies were derived through higher sensitivity in the combined read over the individual interpretations (82% for combined vs 56%, 56%, 65% for DCE, rest, and cine, respectively) and lower specificity in the combined read compared with the individual interpretation (83% combined vs 90%, 89%, 87% for DCE, rest, and cine, respectively). When analyzing various combinations of 2 techniques in a per-vessel analysis, no combination was significantly different from the others. Example CT images and corresponding SPECT and invasive angiography, when applicable, are shown for patients with proven infarcts (Fig. 2 and Fig. 3) and in a patient without any evidence of infarct (Fig. 4).

Image quality and reader confidence

Table 3 summarizes the readers' subjective ratings of image quality and diagnostic confidence for the delayed, rest, and cine images. Readers' assessment of image quality and confidence both tended to be lower for the delayed and cine images when interpretations were "incorrect" (ie, false positive or false negative) compared with "correct" (ie, true positive or true negative). Readers' assessment of rest image quality and confidence showed no statistical difference between correct and incorrect interpretations.

Scan parameters

The mean tube voltages for the cine, rest, and delayed scans were 117 ± 7 kV, 117 ± 7 kV, and 100 ± 4 kV with corresponding mean tube currents of 332 ± 36 mA, 195 ± 42 mA, and 189 ± 24 mA. The average radiation dose during the stress, rest, and delayed scans were DLPs of 601 ± 236 mGy $ cm, 134 ± 39 mGy $ cm, and 74 ± 20 mGy $ cm, respectively, for a total average DLP of 805 mGy $ cm. The average heart rates for the stress, rest, and delayed scans were 76, 65, and 65 beats/min, respectively.

Window width and level

Readers preferred a relatively narrow display window width and level for interpretation, which varied slightly for each case but maintained ratios of window width to level between 0.7 and 1.8 for the delayed images and between 0.6 and 2.1 for the rest images. The average preferred windows for delayed images were width of 208 ± 58, level of 155 ± 30, and a ratio of 1.3 ± 0.2, and for rest images readers preferred window width of 230 ± 58, level of 131 ± 37, and a ratio of 1.4 ± 0.3.

Contrast-to-noise ratio

CNRs were calculated with measurements of CT attenuation in areas of delayed enhancement on the delayed images, along with CT attenuations in remote normal myocardium and in the LV cavity. The mean CNR for abnormal delayed enhancement was 1.63. This analysis was performed only in the 22 cases that were interpreted as positive for infarct on delayed images. The mean attenuation was 85 HU for remote myocardium, 119 HU for the LV cavity, and 111 HU in the areas of delayed enhancement.

Discussion

In this analysis, a comprehensive CT viability protocol showed high accuracy for the detection of infarct compared with the universal definition of MI. We demonstrated that a combined interpretation of all techniques of CT imaging, including wall motion, rest perfusion, and delayed enhancement, was more accurate (90% per patient, 83% per vessel) for the detection of MI than each of the individual phases when assessed alone. However, the findings of delayed enhancement combined with cine wall motion images were nearly as accurate (85%) on a per-patient level and were more sensitive (92%). These findings suggest cardiac CT is a feasible method to accurately detect prior MI in patients with a high probability of CAD compared with the AHA 2007 universal definition.

Others have previously evaluated the use of CT for the detection of MI in both the acute and chronic setting and separately against a histologic "gold standard" in animal models.[18,32,33] Although the AHA universal definition for MI is currently widely used in clinical research,[28] the single imaging test with the best diagnostic profile is late gadolinium enhancement during cardiac MRI.[24] However, MRI is sometimes contraindicated for a number of reasons, including the presence of a pacemaker/defibrillator, claustrophobia, or if local expertise is not available. Conversely, cardiac CT is more widely available and can be rapidly performed and interpreted, particularly if clinical information about coronary stenosis detection is needed.

Other studies have established that CT can detect acute MIs[6] and have evaluated CT and MRI versus histologic samples.[31,33] RPDs usually represent MIs and can frequently be detected with a routine CTA protocol, which is performed during first-pass bolus injection of contrast.[34] Therefore, no incremental radiation expense is associated with a search for MI on routine CTA examinations. However, our research shows that incremental increases in radiation dose for a combined protocol are small. For example, in addition to a routine 64-detector row cardiac CT (2–10 mSv),[35] cine wall motion images may already have been a part of a protocol, and a prospectively triggered delayed phase acquisition could be obtained with only a small radiation dose increment of 1–2 mSv, as our study has shown. A single-phase protocol that uses rest cine imaging (such as a standard retrospectively gated cardiac CTA) or acquisition of only a delayed cine phase (with a larger dose of contrast) could be implemented. This would allow for the combination of wall motion and either resting perfusion defect or delayed contrast enhancement, with a lower total radiation dose (3–9 mSv with the use of modern cardiac-capable CT scanners).[35]

An important caveat is that the imaging "gold standard" for MI, DCE (late gadolinium enhancement) by cardiac MRI, was not available in any of these subjects. Readings that were classified as false positive by CT may have simply been subtle findings that were not detectable by other modalities or not captured in the clinical parameters that define the AHA universal definition for MI. The only reference standard imaging modality that was available in all patients was SPECT, which has lower spatial resolution than CT.[36]

Although our results are promising, at times we encountered difficulties because of the necessarily limited radiation doses, particularly in patients with large body habitus. This low dose was accomplished by the use of low kilovolts and milliamperes, when possible, and also by the use of prospective triggering. Each of these compromises caused artifacts (the former causing noise and worsening beam hardening, the latter causing slab artifacts) that can be decreased when using scanners with longer z-axis detector arrays, stronger tube currents, and iterative reconstruction techniques that are now becoming available on late-generation single- and dual-source scanners. Further, contrast doses necessary to visualize DCE appear to be greater than those necessary for CTA, and we adjusted our protocol to use approximately 140–150 mL of contrast while maintaining a delay time of ~10 minutes.

In addition, because the rest scans were done after the stress scans, there is a possibility of late contrast enhancement contaminating the RPDs and thus decreasing sensitivity for

infarcts on rest imaging. Tube potential setting changes result in differing attenuation values after contrast application; this may limit the quantitative measures and resulting conclusions.

In conclusion, we demonstrated that a comprehensive cardiac CT protocol with 3 phases showed incremental accuracy and sensitivity for infarct detection beyond that of any single phase. However, the specificity of comprehensive analysis versus single analyses was not significantly different. These findings may have implications when designing a clinical CT protocol for detecting infarct.

Acknowledgments

We thank the referring cardiologists of The Massachusetts General Hospital, the Nuclear Medicine Department, and the CT Department and technologists.

We acknowledge the many collaborators who assisted in the collection of this data, including Shanmugam Uthamalingam, MD, Michiel Sala, BS, Nicola K. Drzezga, RT, David Okada, BA, Leon Shturman, DO, Ian Rogers, MD, MPH, Ammar Sarwar, MD, Anand V. Soni, MD, Hiram Bezerra, MD, Milena Petranovic, MD, Ricardo Loureiro, MD, Gudrun Feuchtner, MD, Henry Gewirtz, MD, Amparo Figuero, MD, Otavio Coelho, MD, Udo Hoffmann, MD, MPH, and Wilfred S. Mamuya, MD, PhD.

This study was supported in part by a grant from Astellas Pharma, Inc, the National Institutes of Health (grant 1T32 HL076136 to Drs. Blankstein and Ghoshhajra), from RSNA 213740 (Dr. Ghoshhajra), and Astellas, Pharma, Inc (Dr. Cury).

The authors maintained full control of the study design and data.

The use of adenosine and contrast for cardiac CT are off-label uses.

References

1. Budoff MJ, Dowe D, Jollis JG, Gitter M, Sutherland J, Halamert E, Scherer M, Bellinger R, Martin A, Benton R, Delago A, Min JK: Diagnostic performance of 64-multidetector row coronary computed tomographic angiography for evaluation of coronary artery stenosis in individuals without known coronary artery disease: results from the prospective multicenter ACCURACY (Assessment by Coronary Computed Tomographic Angiography of Individuals Undergoing Invasive Coronary Angiography) trial. J Am Coll Cardiol. 2008;52:1724–32. [PubMed: 19007693]
2. Miller JM, Rochitte CE, Dewey M, Arbab-Zadeh A, Niinuma H, Gottlieb I, Paul N, Clouse ME, Shapiro EP, Hoe J, Lardo AC, Bush DE, de Roos A, Cox C, Brinker J, Lima JAC: Diagnostic performance of coronary angiography by 64-row CT. N Engl J Med. 2008; 359:2324–36. [PubMed: 19038879]
3. Okada D, Ghoshhajra BB, Blankstein R, Rocha-Filho JA, Shturman L, Rogers IS, Bezerra H, Sarwar A, Gewirtz H, Hoffmann U, Mamuya W, Brady T, Cury R: Direct comparison of rest and adenosine stress myocardial perfusion CT with rest and stress SPECT. J Nucl Cardiol. 2010;17:27–37. [PubMed: 19936863]
4. Blankstein R, Shturman LD, Rogers IS, Rocha-Filho JA, Okada DR, Sarwar A, Soni AV, Bezerra H, Ghoshhajra BB, Petranovic M, Loureiro R, Feuchtner G, Gewirtz H, Hoffmann U, Mamuya WS, Brady TJ, Cury RC: Adenosine-induced stress myocardial perfusion imaging using dual-source cardiac computed tomography. J Am Coll Cardiol. 2009;54:1072–84. [PubMed: 19744616]
5. George RT, Arbab-Zadeh A, Miller JM, Kitagawa K, Chang H-J, Bluemke DA, Becker L, Yousuf O, Texter J, Lardo AC, Lima JAC: Adenosine stress 64- and 256-row detector computed tomography angiography and perfusion imaging: a pilot study evaluating the transmural extent of perfusion abnormalities to predict atherosclerosis causing myocardial ischemia. Circ Cardiovasc Imaging. 2009;2:174–82. [PubMed: 19808590]
6. Cury RC, Nieman K, Shapiro MD, Butler J, Nomura CH, Ferencik M, Hoffmann U, Abbara S, Jassal DS, Yasuda T, Gold HK, Jang IK, Brady TJ: Comprehensive assessment of myocardial

perfusion defects, regional wall motion, and left ventricular function by using 64-section multidetector CT. Radiology. 2008;248:466–75. [PubMed: 18641250]

7. Henneman MM, Bax JJ, Schuijf JD, Jukema JW, Holman ER, Stokkel MPM, Lamb HJ, de Roos A, van der Wall EE: Global and regional left ventricular function: a comparison between gated SPECT, 2D echocardiography and multi-slice computed tomography. Eur J Nucl Med Mol Imaging. 2006;33:1452–60. [PubMed: 16865394]
8. Nieman K, Cury RC, Ferencik M, Nomura CH, Abbara S, Hoffmann U, Gold HK, Jang I-K, Brady TJ: Differentiation of recent and chronic myocardial infarction by cardiac computed tomography. Am J Cardiol. 2006;98:303–8. [PubMed: 16860013]
9. Nikolaou K, Sanz J, Poon M, Wintersperger BJ, Ohnesorge B, Rius T, Fayad ZA, Reiser MF, Becker CR: Assessment of myocardial perfusion and viability from routine contrast-enhanced 16-detector-row computed tomography of the heart: preliminary results. Eur Radiol. 2005;15:864–71. [PubMed: 15776243]
10. Mendoza DD, Joshi SB, Weissman G, Taylor AJ, Weigold WG: Viability imaging by cardiac computed tomography. J Cardiovasc Comput Tomogr. 2010;4:83–91. [PubMed: 20430338]
11. Axsom K, Lin F, Weinsaft JW, Min JK: Evaluation of myocarditis with delayed-enhancement computed tomography. J Cardiovasc Comput Tomogr. 2009;3:409–11. [PubMed: 20083062]
12. Baks T, Cademartiri F, Moelker AD, Weustink AC, van Geuns R-J, Mollet NR, Krestin GP, Duncker DJ, de Feyter PJ: Multislice computed tomography and magnetic resonance imaging for the assessment of reperfused acute myocardial infarction. J Am Coll Cardiol. 2006; 48:144–52. [PubMed: 16814660]
13. Chang HJ, George RT, Schuleri KH, Evers K, Kitagawa K, Lima JAC, Lardo AC: Prospective electrocardiogram-gated delayed enhanced multidetector computed tomography accurately quantifies infarct size and reduces radiation exposure. JACC Cardiovasc Imaging. 2009;2:412–20. [PubMed: 19580722]
14. Mahnken AH, Bruners P, Mühlenbruch G, Emmerich M, Hohl C, Günther RW, Wildberger JE: Low tube voltage improves computed tomography imaging of delayed myocardial contrast enhancement in an experimental acute myocardial infarction model. Invest Radiol. 2007; 42:123–9. [PubMed: 17220730]
15. Ichikawa Y, Kitagawa K, Chino S, Ishida M, Matsuoka K, Tanigawa T, Nakamura T, Hirano T, Takeda K, Sakuma H: Adipose tissue detected by multislice computed tomography in patients after myocardial infarction. JACC Cardiovasc Imaging. 2009;2:548–55. [PubMed: 19442939]
16. Baroldi G, Silver MD, De Maria R, Parodi O, Pellegrini A: Lipomatous metaplasia in left ventricular scar. Can J Cardiol. 1997;13:65–71. [PubMed: 9039067]
17. Su L, Siegel JE, Fishbein MC: Adipose tissue in myocardial infarction. Cardiovasc Pathol. 2004;13:98–102. [PubMed: 15033159]
18. Blankstein R, Rogers IS, Cury RC: Practical tips and tricks in cardiovascular computed tomography: diagnosis of myocardial infarction. J Cardiovasc Comput Tomogr. 2009;3:104–11. [PubMed: 19332342]
19. Jacobi AH, Gohari A, Zalta B, Stein MW, Haramati LB: Ventricular myocardial fat: CT findings and clinical correlates. J Thorac Imaging. 2007;22:130–5. [PubMed: 17527115]
20. Cury RC, Cattani CAM, Gabure LAG, Racy DJ, de Gois JM, Siebert U, Lima SS, Brady TJ: Diagnostic performance of stress perfusion and delayed-enhancement MR imaging in patients with coronary artery disease. Radiology. 2006;240:39–45. [PubMed: 16793971]
21. Nagel E, Lima JAC, George RT, Kramer CM: Newer methods for non-invasive assessment of myocardial perfusion: cardiac magnetic resonance or cardiac computed tomography? JACC Cardiovasc Imaging. 2009;2:656–60. [PubMed: 19442955]
22. Lee DC, Simonetti OP, Harris KR, Holly TA, Judd RM, Wu E, Klocke FJ: Magnetic resonance versus radionuclide pharmacological stress perfusion imaging for flow-limiting stenoses of varying severity. Circulation. 2004;110:58–65. [PubMed: 15210596]
23. Schwitter J, Wacker CM, van Rossum AC, Lombardi M, Al-Saadi N, Ahlstrom H, Dill T, Larsson HB, Flamm SD, Marquardt M, Johansson L: MR-IMPACT: comparison of perfusion-cardiac magnetic resonance with single-photon emission computed tomography for the detection of

coronary artery disease in a multicentre, multivendor, randomized trial. Eur Heart J. 2008;29:480–9. [PubMed: 18208849]

24. Taylor AJ, Cerqueira M, Hodgson JM, Mark D, Min J, O'Gara P, Rubin GD, American College of Cardiology Foundation Appropriate Use Criteria Task Force; Society of Cardiovascular Computed Tomography; American College of Radiology; American Heart Association; American Society of Echocardiography; American Society of Nuclear Cardiology; North American Society for Cardiovascular Imaging; Society for Cardiovascular Angiography and Interventions; Society for Cardiovascular Magnetic Resonance, Kramer CM, Berman D, Brown A, Chaudhry FA, Cury RC, Desai MY, Einstein AJ, Gomes AS, Harrington R, Hoffmann U, Khare R, Lesser J, McGann C, Rosenberg A, Schwartz R, Shelton M, Smetana GW, Smith SC Jr.: ACCF/SCCT/ACR/AHA/ASE/ASNC/NASCI/SCAI/SCMR 2010 appropriate use criteria for cardiac computed tomography. A report of the American College of Cardiology Foundation Appropriate Use Criteria Task Force, the Society of Cardiovascular Computed Tomography, the American College of Radiology, the American Heart Association, the American Society of Echocardiography, the American Society of Nuclear Cardiology, the North American Society for Cardiovascular Imaging, the Society for Cardiovascular Angiography and Interventions, and the Society for Cardiovascular Magnetic Resonance. J Am Coll Cardiol. 2010;56:1864–94. [PubMed: 21087721]
25. McCollough CH, Primak AN, Saba O, Bruder H, Stierstorfer K, Raupach R, Suess C, Schmidt B, Ohnesorge BM, Flohr TG: Dose performance of a 64-channel dual-source CT scanner. Radiology. 2007; 243:775–84. [PubMed: 17446525]
26. Achenbach S, Ropers U, Kuettner A, Anders K, Pflederer T, Komatsu S, Bautz W, Daniel WG, Ropers D: Randomized comparison of 64-slice single- and dual-source computed tomography coronary angiography for the detection of coronary artery disease. JACC Cardiovasc Imaging. 2008;1:177–86. [PubMed: 19356426]
27. Ropers U, Ropers D, Pflederer T, Anders K, Kuettner A, Stilianakis NI, Komatsu S, Kalender W, Bautz W, Daniel WG, Achenbach S: Influence of heart rate on the diagnostic accuracy of dual-source computed tomography coronary angiography. J Am Coll Cardiol. 2007;50:2393–8. [PubMed: 18154964]
28. Thygesen K, Alpert JS, White HD; Joint ESC/ACCF/AHA/WHT Task Force for the Redefinition of Myocardial Infarction, Jaffe AS, Apple FS, Galvani M, Katus HA, Newby LK, Ravkilde J, Chaitman B, Clemmensen PM, Dellborg M, Hod H, Porela P, Underwood R, Bax JJ, Beller GA, Bonow R, Van der Wall EE, Bassand J-P, Wijns W, Ferguson TB, Steg PG, Uretsky BF, Williams DO, Armstrong PW, Antman EM, Fox KA, Hamm CW, Ohman EM, Simoons ML, Poole-Wilson PA, Gurfinkel EP, Lopez-Sendon J-L, Pais P, Mendis S, Zhu J-R, Wallentin LC, Fern ández-Avilés F, Fox KM, Parkhomenko AN, Priori SG, Tendera M, Voipio-Pulkki L-M, Vahanian A, Camm AJ, De Caterina R, Dean V, Dickstein K, Filippatos G, Funck-Brentano C, Hellemans I, Kristensen SD, McGregor K, Sechtem U, Silber S, Tendera M, Widimsky P, Zamorano JL, Morais J, Brener S, Harrington R, Morrow D, Lim M, Martinez-Rios MA, Steinhubl S, Levine, Gibler WB, Goff D, Tubaro M, Dudek D, Al-Attar N: Universal definition of myocardial infarction. Circulation. 2007;116:2634–53. [PubMed: 17951284]
29. Rocha-Filho JA, Blankstein R, Shturman LD, Bezerra HG, Okada DR, Rogers IS, Ghoshhajra B, Hoffmann U, Feuchtner G, Mamuya WS, Brady TJ, Cury RC: Incremental value of adenosine-induced stress myocardial perfusion imaging with dual-source CT at cardiac CT angiography. Radiology. 2010;254:410–9. [PubMed: 20093513]
30. Cerqueira MD, Weissman NJ, Dilsizian V, Jacobs AK, Kaul S, Laskey WK, Pennell DJ, Rumberger JA, Ryan T, Verani MS, American Heart Association Writing Group on Myocardial Segmentation and Registration for Cardiac Imaging: Standardized myocardial segmentation and nomenclature for tomographic imaging of the heart: a statement for healthcare professionals from the Cardiac Imaging Committee of the Council on Clinical Cardiology of the American Heart Association. Circulation. 2002;105:539–42. [PubMed: 11815441]
31. Gerber BL, Belge B, Legros GJ, Lim P, Poncelet A, Pasquet A, Gisellu G, Coche E, Vanoverschelde J-LJ: Characterization of acute and chronic myocardial infarcts by multidetector computed tomography: comparison with contrast-enhanced magnetic resonance. Circulation. 2006;113:823–33. [PubMed: 16461822]
32. Chang H-J, George RT, Schuleri KH, Evers K, Kitagawa K, Lima JAC, Lardo AC: Prospective electrocardiogram-gated delayed enhanced multidetector computed tomography accurately

quantifies infarct size and reduces radiation exposure. JACC Cardiovasc Imaging. 2009;2:412–20. [PubMed: 19580722]

33. Lardo AC, Cordeiro MAS, Silva C, Amado LC, George RT, Saliaris AP, Schuleri KH, Fernandes VR, Zviman M, Nazarian S, Halperin HR, Wu KC, Hare JM, Lima JAC: Contrast-enhanced multidetector computed tomography viability imaging after myocardial infarction: characterization of myocyte death, microvascular obstruction, and chronic scar. Circulation. 2006;113:394–404. [PubMed: 16432071]
34. George RLA: Infarct detection or infarct characterization? Noncontrast CT and its implications for characterizing chronic myocardial scar. J Cardiovasc Comput Tomogr. 2010;4:108–9. [PubMed: 20430340]
35. Alkadhi H, Stolzmann P, Scheffel H, Desbiolles L, Baumüller S, Plass A, Genoni M, Marincek B, Leschka S: Radiation dose of cardiac dual-source CT: the effect of tailoring the protocol to patient-specific parameters. Eur J Radiol. 2008;68:385–91. [PubMed: 18976876]
36. Ono H, Funabashi N, Uehara M, Yahima R, Kataoka A, Ueda M, Miyauchi H, Daimon M, Takaoka H, Komuro I: Comprehensive evaluation of characteristics of left ventricular myocardium in a subject with non-coronary arterial cardiac dysfunction through segment by segment analysis using various diagnostic modalities. Int J Cardiol. 2010;125:95–100.

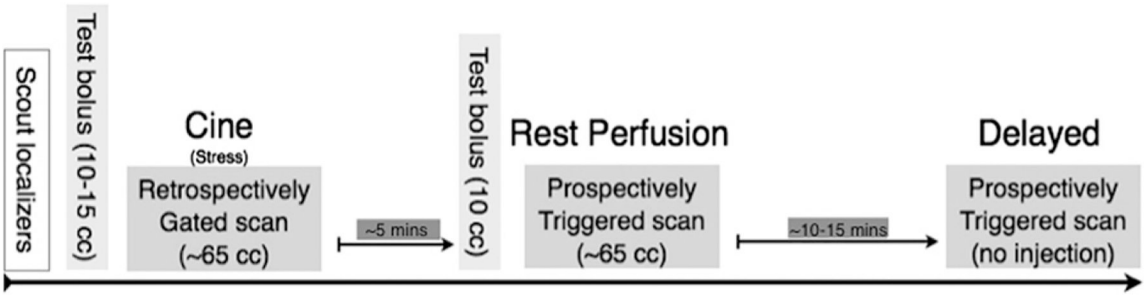

Figure 1.

Comprehensive infarct detection protocol. After scout and localizer images were obtained, contrast-enhanced cine imaging (retrospective ECG gating with tube current modulation) was obtained (this was performed during adenosine stress, but myocardial stress perfusion images were not used in the present analysis). Approximately 5 minutes later, prospectively ECG-triggered rest perfusion images were obtained during a second contrast bolus infusion. Approximately 10–15 minutes later, prospectively ECG-triggered delayed images were obtained, without additional contrast for myocardial delayed enhancement imaging.

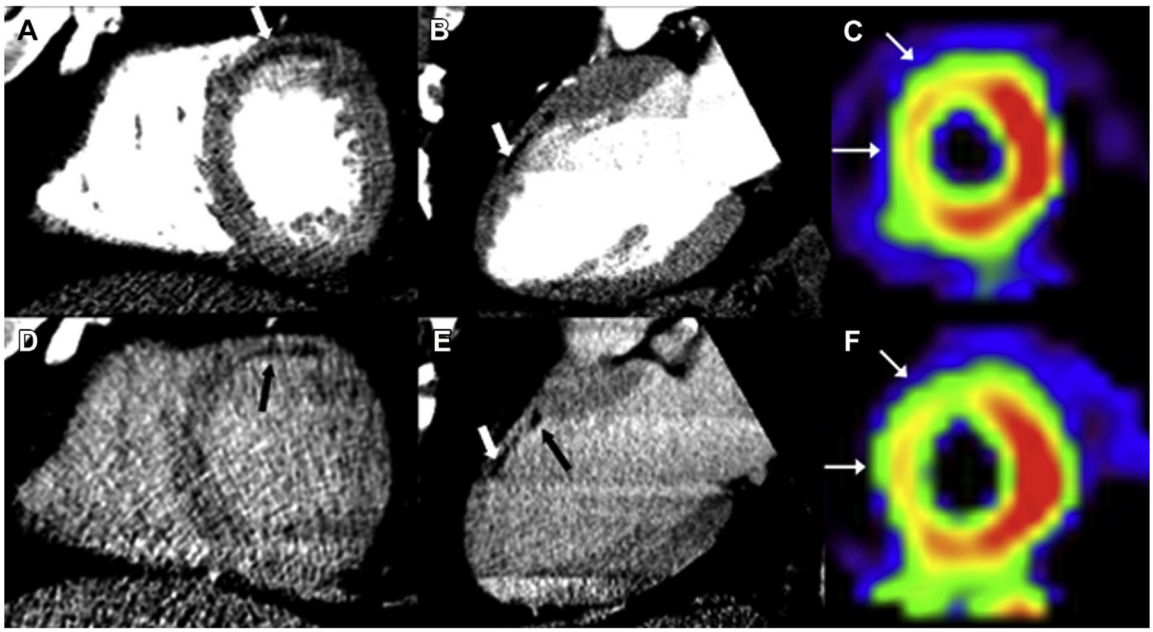

Figure 2.

Chronic myocardial infarction. Rest (**A** and **B**) and delayed (**D** and **E**) CT images from a 59-year-old man with a history of prior myocardial infarction, dyslipidemia, and hypertension show a chronic infarct in the territory of the left anterior descending artery in the anterior wall. Areas of hypoenhancement (*white arrow*, images **A** and **E**) suggest the presence of fatty metaplasia, also in the anterior wall. In addition to fat in the anterior wall, abnormal contrast enhancement (*black arrows*, images **D** and **E**) is present on delayed images in the subendocardium of the anterior wall. SPECT imaging at stress (**C**) and rest (**F**) of the same patient shows a fixed perfusion defect along the anteroseptal wall (*white arrows*).

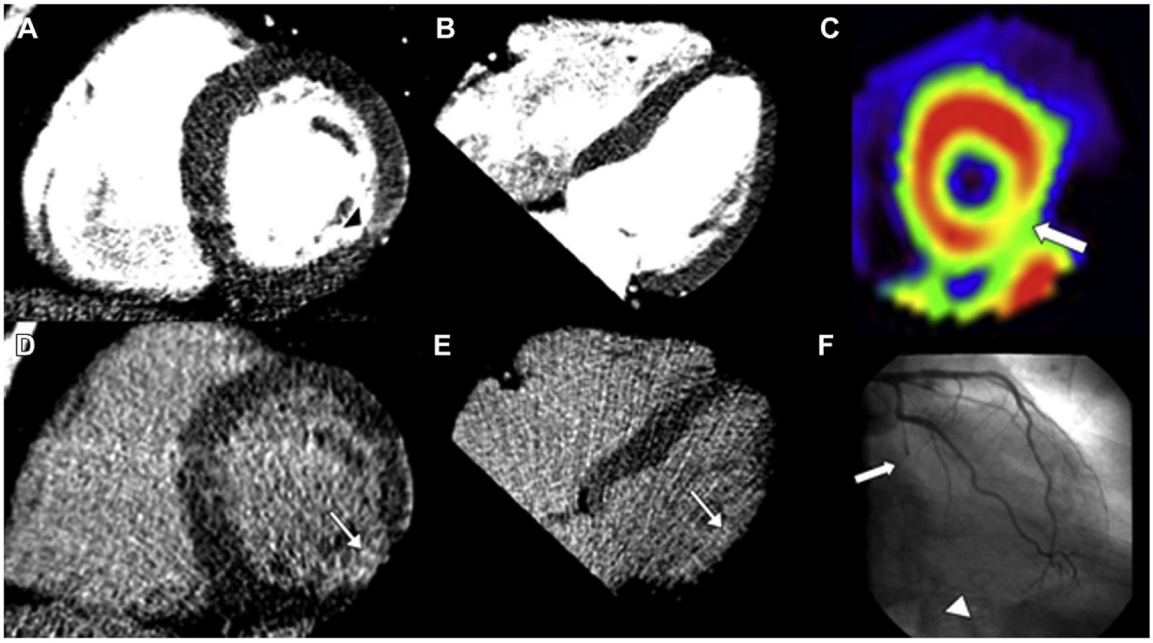

Figure 3.

Circumflex infarct. Cardiac CT images (**A**, **B**, **D**, and **E**), SPECT (**C**), and invasive angiography (**F**) of a 63-year-old man with a history of dyslipidemia, myocardial infarction, and percutaneous coronary intervention (left circumflex, left anterior descending, diagonal branch). Regional myocardial thinning in the lateral wall (*black arrowhead*) on the rest images (**A** and **B**) and abnormal late contrast enhancement (*white arrow*) on the delayed images (**D** and **E**) indicate the presence of infarction in the circumflex territory (inferolateral wall). The SPECT image of the short axis of the left ventricle shows moderate ischemia in the inferolateral wall (**C**; *white arrow*). The angiogram shows occlusion of the mid circumflex (**F**; *white arrow*) and filling of distal collaterals (*arrowhead*).

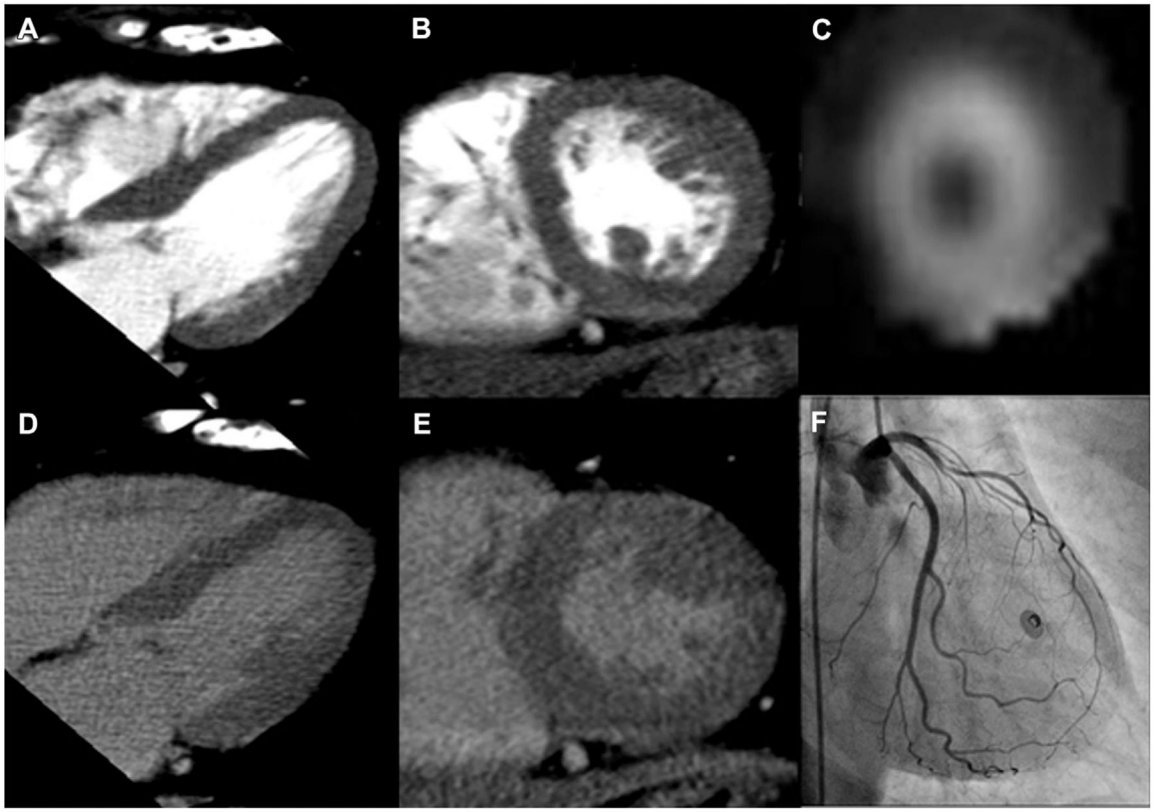

Figure 4.

Normal examination. Cardiac CT (**A**, **B**, **D**, and **E**), SPECT (**C**), and invasive angiography (**F**) images from a 56-year-old woman with history of dyslipidemia, smoking, and family history of CAD, but no history of infarct. Rest images (**A** and **B**) and delayed images (**D** and **E**) are shown in long-axis (**A** and **D**) and short-axis (**B** and **E**) views that are both used for interpretation, according to the AHA standardized myocardial segmentation. SPECT image in the short axis of the left ventricle (**C**) shows normal perfusion at rest, whereas angiography during left main injection shows patency of the left anterior descending, left circumflex, and all major branches.

J Cardiovasc Comput Tomogr. Author manuscript; available in PMC 2020 February 21.

Table 1

Demographics and baseline characteristics

	Patients without reference MI* (n = 24)	Patients with reference MI* (n = 24)	P
Age, mean ± SD, y	61.2 ± 11.0	63.3 ± 10.2	0.35
Male, %	70.8	95.8	0.02
Diabetes mellitus, %	16.7	29.2	0.23
Hypertension, %	83.3	95.8	0.16
Dyslipidemia, %	79.2	100	0.02
Obesity (BMI > 30 kg/m^2), %	37.5	54.2	0.25
Smoking history, %	66.7	66.7	0.999
Ethnicity, %			
White	83.3	83.3	0.999
Black	12.5	12.5	0.999
Hispanic	4.2	4.2	0.999
Prior medical history, %			
Previous angina	54.2	58.3	0.77
Prior myocardial infarction *	12.5	58.3	<0.001
Peripheral vascular disease	12.5	4.2	0.30
Prior CVA	0.0	0	NA
Prior coronary revascularization	20.8	54.2	0.02
Biomarkers/lipids, mean ± SD, mg/dL			
Total cholesterol	191.1 ± 53.0	157.0 ± 42.2	0.15
HDL cholesterol	50.3 ± 20.9	41.9 ± 12.1	0.16
LDL cholesterol	115.5 ± 54.6	88.9 ± 28.8	0.11
Serum triglycerides	159.4 ± 54.8	151.3 ± 122.3	0.44
Serum creatinine	1.1 ± 0.2	1.1 ± 0.2	0.49
Baseline medications, %			
Aspirin	58.3	70.8	0.37
β-Blocker	66.7	83.3	0.18
Statin	62.5	91.7	0.02
Vital signs			

	Patients without reference MI* (n = 24)	Patients with reference MI* (n = 24)	P
Heart rate, mean ± SD, beats/min	66.4 ± 11.6	64.0 ± 11.7	0.41
Systolic BP, mean ± SD, mm Hg	141.8 ± 19.8	139 ± 9.4	0.49
Diastolic BP, mean ± SD, mm Hg	78.6 ± 9.9	79.8 ± 9.7	0.44

Reference MI, myocardial infarction according to 2007 AHA universal definition; HDL, high-density lipoprotein; LDL, low-density lipoprotein. Family history, diabetes, and dyslipidemia were classified according to documentation in the cardiologist's notes.

*Prior myocardial infarction was based on past notes in patient's chart, not according to the 2007 AHA guidelines used for the reference MI.

J Cardiovasc Comput Tomogr. Author manuscript; available in PMC 2020 February 21.

Table 2

Diagnostic accuracy of CT protocol versus reference MI per patient and per vessel

	Sensitivity, % (95% CI)	Specificity, % (95% CI)	PPV, % (95% CI)	NPV, % (95% CI)	Accuracy, % (95% CI)
Per patient					
DCE	79 (58–93)	88 (68–97)	86 (65–97)	81 (61–93)	83 (70–93)
Rest	67 (45–84)	92 (73–99)*	89 (65–97)	73 (54–88)	79 (65–90)
Cine	79 (58–93)	88 (68–97)	86 (65–97)	81 (61–93)	83 (70–93)
Combined interpretation	88 (68–97)	92 (73–99)*	91 (72–99)*	88 (69–97)	90 (77–97)*
DCE + cine	92 (73–99)*	79 (58–93)	81 (62–94)	90 (70–99)*	85 (72–94)
Rest + cine	83 (63–95)	79 (58–93)	80 (59–93)	83 (61–95)	81 (67–91)
Rest + DCE	83 (63–95)	83 (63–95)	83 (63–95)	83 (63–95)	83 (70–93)
Per vessel					
DCE	56 (38–73)	90 (83–95)*	63 (44–80)*	87 (79–92)	82 (75–88)
Rest	56 (38–73)	89 (82–94)	61 (42–78)	87 (79–92)	81 (74–87)
Cine	65 (46–80)	87 (80–93)	61 (43–77)	89 (81–94)	82 (75–88)
Combined interpretation	82 (65–93)*	83 (74–89)	60 (44–74)	94 (87–98)*	83 (75–88)*
DCE + cine	71 (53–85)	83 (74–89)	56 (40–71)	90 (83–95)	80 (72–86)
Rest + cine	74 (56–87)	81 (72–88)	54 (39–69)	91 (83–96)	79 (72–85)
Rest + DCE	74 (56–87)	85 (76–91)	60 (43–71)	91 (84–96)	82 (75–88)
SPECT	85 (69–95)	97 (92–99)	91 (75–98)	96 (90–99)	94 (89–98)

PPV, positive predictive value; NPV, negative predictive value.

*Highest value.

Table 3

Image quality and confidence

	Consensus	True positive or true negative	False positive or false negative	P
Delayed IQ	2.5	2.6	2.1	0.02
Rest IQ	3.0	3.0	3.1	0.92
Cine IQ	3.0	3.1	2.7	0.08
Delayed confidence	2.8	2.8	2.4	0.05
Rest confidence	2.9	2.8	2.9	0.88
Cine confidence	3.1	3.2	2.7	0.04

Ratings are subjective, on a scale from 1 to 4, with 1 being the lowest degree of confidence and 4 being the highest degree of confidence.